

Development of an Ejectable Data Recorder Ejection Mechanism for the Low-Earth Orbit Flight Test of an Inflatable Decelerator

Brian Saulman* and Robert Wagner**

Abstract

On November 10, 2022, the 1100kg (2,425 lbs.) Low-Earth Orbit Flight Test of an Inflatable Decelerator (LOFTID) Reentry Vehicle (RV) was launched on a United Launch Alliance (ULA) Atlas V as a secondary payload with the Joint Polar Surveyor System-2. The 6-meter diameter (~20 ft.) aeroshell (a type of heat shield) entered the atmosphere at 8 kilometers per second (18,000 miles per hour), flew nominally, enduring the intended heat pulse that saw temperatures exceeding 1371°C (2500°F) on the front side while the payload skin remained only about 38°C (100°F) before landing under parachute in the Pacific Ocean off the coast of Hawaii. The RV exceeded Mach 30 and the heat-affected aeroshell withstood a pressure pulse that exerted 9g's deceleration maintaining stable flight through the hypersonic, supersonic, transonic, and subsonic regimes to the parachute deployment. As part of the Agency's strategic goal "to extend human presence deeper into space and to the moon for sustainable long-term exploration and utilization", the LOFTID inflatable aerodynamic decelerator or aeroshell technology could one day help land humans on Mars.

As with any flight test, data collection is of utmost importance. Without a data downlink from the RV and a possibility of the RV sinking before the recovery crew got to it, a secondary data collection method was introduced. The RV would eject an ejectable data recorder (EDR), which would have a duplicate copy of the on-board flight data, before splashdown and be retrieved separately.

This paper discusses the development of the ejection mechanism used to eject the data recorder from the RV during the test flight.

Introduction

The LOFTID RV was designed such that there was no data downlink to receive flight data in real time. With the very real possibility of the RV sinking after splashdown, a secondary means of retrieving the flight data was conceived. The EDR was developed to accomplish this. While it resides on-board the RV during flight, it received a copy of the flight data along with a similar unit that remained within the vehicle, but the EDR would be projected out away from the RV during decent and splashdown in the Pacific Ocean to be recovered up to thirty days later after ejection. To project the EDR from the RV, the EDR ejection mechanism was developed. Throughout the development, the mechanism had many constraints and challenges which will be discussed in this paper.

EDR Ejection Mechanism Background

The LOFTID RV consists of an inflatable soft goods structure and a metallic center body structure, Figure 1. The center body consists of three segments: forward, mid, and aft, Figure 2. The aft segment was chosen to house EDR ejection mechanism due to its location having the most direct path for an object to clear the inflated aeroshell. This location provided its own set of challenges. The aft segment also housed the parachute system, parachute mortar, and various electronics systems leaving very little space for the ejection mechanism. The location also sat roughly even with the outer torus of the inflatable structure and 2 meters away from it forcing ejection trajectory to be more vertical. Due to space constraints in the aft segment, a 20° off horizontal angle was selected for ejection path, Figure 3.

* NASA Langley Research Center, Hampton, VA

** NASA Langley Research Center, Science and Technology Corporation, Hampton, VA

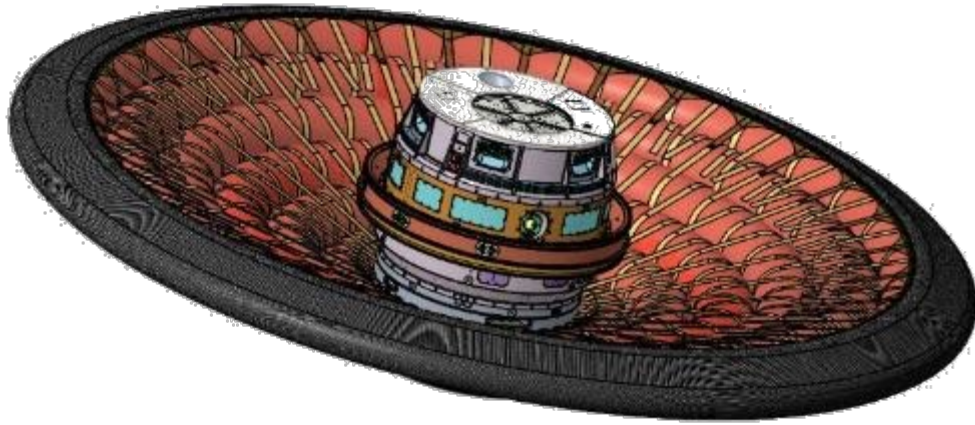


Figure 1. LOFTID RV in Flight Configuration

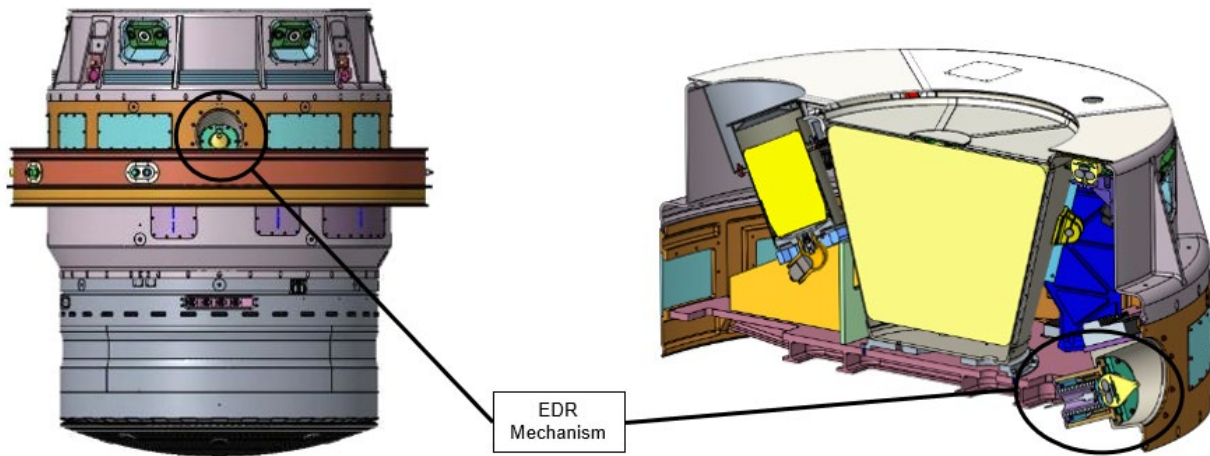


Figure 2. LOFTID Center Body and EDR Mechanism Location

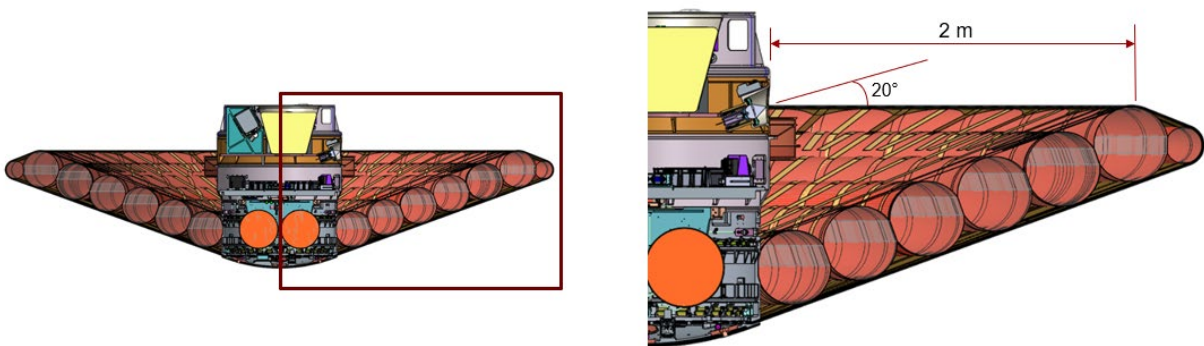


Figure 3. LOFTID RV Flight Configuration and EDR Mechanism Location

The ejection system was to eject the Ejectable Data Module (EDM), Figure 4, through the RV boundary layer and clear the vehicle during decent. The EDM was a pear-shaped polyurethane cast assembly that

contained data storage, Iridium and Long Range (LoRA) broadcast networks, and batteries to survive at least thirty days in the ocean. The EDM weighed only 165 grams (0.364 lbs.) and constrained the ejection system to impart a maximum acceleration of 200g's into it which limited how much force could be used to eject it.



Figure 4. Ejectable Data Module

EDR Ejection Mechanism Design and Analysis Overview

The ejection mechanism is a bolted assembly consisting of housing components, compression spring, EDM pusher with tungsten disulfide dry film lubricant, guide pins, non-explosive actuator (NEA), elastomeric bumper, EDM, EDM interface board (EDMIB), shield, and a flexible thermal protective system (FTPS), Figure 5. A bushing and closeout plates were added later in the design cycle due to test findings that will be discussed later.

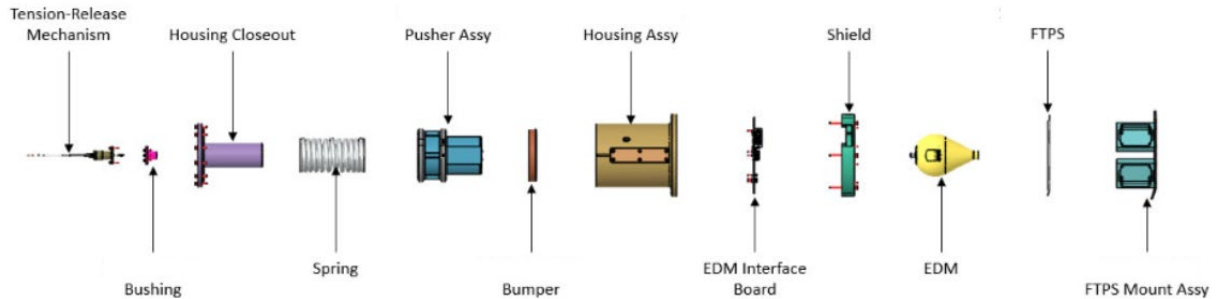


Figure 5. Ejection Mechanism Components

Using MSC.ADAMS, a dynamics model was constructed to account for the relative motion of the RV; this motion is like a spinning top— as the RV spins about the roll axis, the RV tilts in a sinusoidal motion about the pitch and yaw axes from center-of-gravity of the RV. As illustrated in Figure 6, the EDM is located approximately on the same horizontal plane as the top of the RV toroid. As mentioned previously, the housing of the EDR is set to a maximum angle of 20°. In the MSC.ADAMS model, the top of the RV toroid is constructed out of rigid beams; therefore, a clearance marker was added to the model to account for the maximum displacement envelope of the flexible toroid structure. Independent testing was performed on the RV aeroshell to baseline displacements against finite element model results.

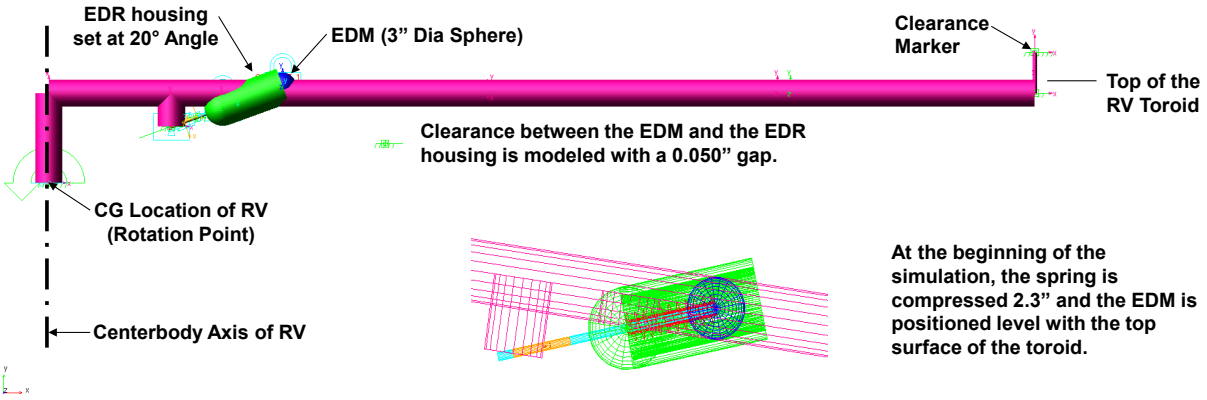


Figure 6. MSC.ADAMS Ejectable Data Recorder Model

Trajectory studies were performed on the RV's reentry. The 2s pitch and yaw angular velocity and angular acceleration rates were derived and supplied for the analysis. With the EDR ejection planned at 50,000 ft, frequencies were calculated for pitch and yaw orientations at elevations ranging from 45,000 ft to 55,000 ft. The natural frequency observed averages nearly 3.485 rad/s and is consistent through 45,000 ft to 55,000 ft, Figure 7.

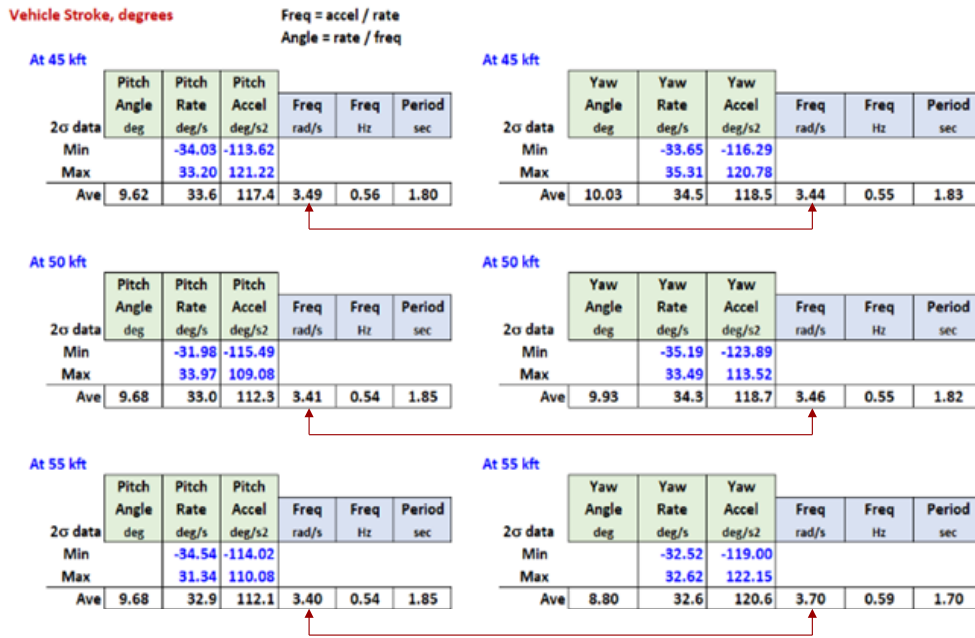


Figure 7. Trajectory Study Data (from 45,000 ft to 50,000 ft)

General motion of the toroid is controlled through the equation for velocity as a function of time. Several simulations were performed by releasing the data module at different time increments with measurements taken from the clearance marker to the EDM as it passes over the edge of the toroid.

In accordance with NASA-STD-5017, a minimum ejection velocity of 30.40 ft/s is needed to maintain a positive force margin of safety. As shown below in Figure 8, the dots along the oval represent each of the individual simulations. The red curve indicates the angular velocity of the RV is upward which is where the smallest clearance is observed.

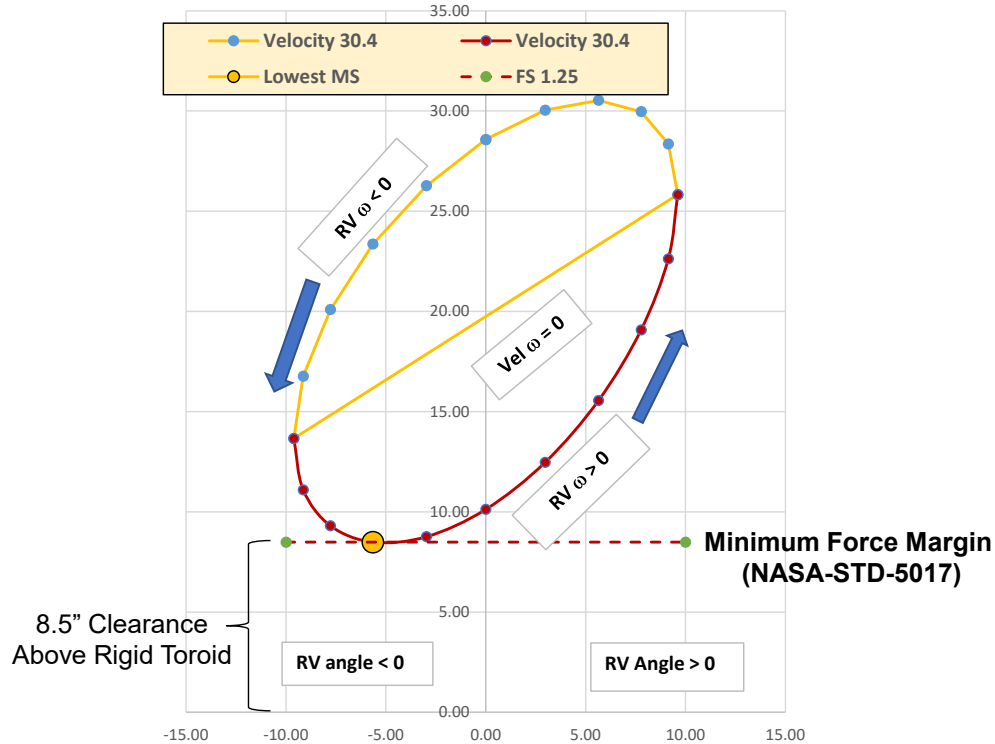


Figure 8. Ejection Velocity at 30.4 ft/s

From the minimum ejection velocity needed, the kinetic energy is calculated and then converted into spring energy per Equation 1.

$$0.5 * m * v^2 = 0.5 * k * x^2$$

Equation 1. Kinetic Energy to Spring Energy

EDR Ejection Mechanism Assembly and Function

The mechanism was a standalone assembly and was installed as late as possible into the RV before encapsulation and assembly onto the booster. Assembly was straight forward. With the bumper already bonded to the inside of the housing, the pusher was placed into the housing. Three dowel pins aligned the pusher to the housing with one of the dowel pins smaller than the other two so the pusher can only be assembled in one orientation. The spring was slid over the housing closeout, inserted into the housing, and bolted to the housing. The interface board and EDM were aligned to the pusher. Two dowel pins oriented the EDM to the pusher. Different sized dowel pins were used again so the EDM could only be oriented one way. Once in place, the interface board was fastened to the housing. All the previous operations only needed to be completed once.

To load the mechanism for ejection, a set of custom retraction screws were threaded through the back of the housing into the pusher. Sprockets and chain were then installed to the retraction screws as this allowed the screws to be turned at the same time with a standard socket wrench, Figure 9. Retraction occurred until the EDM was seated properly into the interface board. Once retracted, safety bolts were installed to prevent inadvertent spring extensions.

A bushing and the NEA, Figure 10, were then installed through the back of the housing. The NEA threaded into the base of the EDM until hand tight and then fastened in place. The retraction screws were then removed preloading the NEA fastener.



Figure 9. Mechanism Retraction



Figure 10. Non-Explosive Actuator

The shield, FTPS mount, and FTPS were then assembled to the forward end of the housing completing the assembly, Figure 11.



Figure 11. EDR Mechanism Assembly

There are two ways to operate the EDR mechanism. For flight, a voltage is applied to the NEA and a bridge wire wrapped around a split spool expands releasing the NEA fastener. For testing or quickly repeating operations, the NEA split spool was replaced with a mechanical release device that could be manually operated by turning it, Figure 12.



Figure 12. NEA Split Spool (Top), Mechanical Release (Bottom)

EDR Developmental Testing

The ejection system relies on a single spring. The compression spring was sized by empirical calculations to calculate the stiffness and the available stroke of the spring. As shown in Figure 13, the candidate spring has a stiffness of 135.8 pounds per inch and a stroke length of 2.3 inches. A calculated force of 312.3 pounds-force is expected when the spring is compressed 2.3 inches.

	17-7 PH Material	Units	Comments
Spring Length,	7.000	in	per Vendor catalogue
Spring Diameter, D_{outer}	2.437	in	per Vendor catalogue
Wire Diameter, d	0.312	in	per Vendor catalogue
Mean Diameter, D	1.813	in	$= D_{outer} - 2 * d$
Mean Diameter, D	2.125	in	$= D_{outer} - d$
Shear Modulus, G	11.0E+06	psi	Material Property Dependent
Number of Total Coils, N	12		per Vendor catalogue
Select Type of End	Closed and Ground	< <input type="checkbox"/> >	
Number of Active Coils, n	10		Ranges for $[N \text{ to } (N-2)]$ based on End Type
Spring Stiffness, k	135.8	lbs/in	$= G * d^4 / (8 * n * D^3)$
Wahl Curvature Stress Correction Factor, K	1.219		$= [4 * (D/d) - 1] / [4 * (D/d) - 4] + [0.615 / (D/d)]$
Beginning of Stroke, δ_{begin}	2.30	in	Mechanical stop used to limit the beginning of stoke.
End of Stroke, δ_{end}	0.00	in	Mechanical stop used to limit the end of stoke.
Stroke Length, δ	2.30	in	$= \delta_{begin} - \delta_{end}$
Wire Shear Stress, τ	67,849	psi	$= 8 * k * D * K * \delta / (\pi * d^3)$
Max. Suggested Stroke, δ_{max}	2.50	in	per Vendor catalogue
Displacement to Reach Solid Height, h	3.256	in	per Vendor catalogue
Spacing between Coils, x	0.271	in	Check: Spacing between coil < wire diameter
Max Operating Spring Force, P_{max}	312.3	lbf	per Vendor catalogue
Material Specification,	ASTM A313		Dual Certified under SAE AMS 5678F
Material Class,	17-7 PH Cond C		Rockwell hardness ranges from C38-C57
Ultimate Tensile Strength, σ_{ult}	192,000	psi	from AMS 5678F, Cond. C (17-7 PH Stainless)
Ultimate Shear Strength, τ_{ult}	128,640	psi	$= 0.67 * \sigma_{ult}$ (R. L. Norton)
Yield Strength, σ_y	163,200	psi	$= 0.85 * \sigma_{ult}$
Shear Yield Strength, τ_y	109,344	psi	$= (\tau_{ult} / \sigma_{ult}) * \sigma_y$
FS for Mission-critical springs, FS_{ult}	1.65		per NASA-STD-5017a (Table 3) Ultimate Strength
FS for Mission-critical springs, FS_{yield}	1.50		per NASA-STD-5017a (Table 3) Yield Strength
Margin of Safety on Ultimate, MS_{ult}	0.15		$= [\tau_{ult} / (FS_{ult} * \tau)] - 1$
Margin of Safety on Yield, MS_{yld}	0.07		$= [\tau_y / (FS_{yld} * \tau)] - 1$

Please note: δ_{max} is a statistical service-life of 100,000 cycles with infrequent breakage ~ Century Spring Corp.

Figure 13. Compression Spring Calculations

Compression testing was performed on the compression spring to vary the theoretical stiffness calculations, Figure 14. The spring slightly exceeded the empirical calculations. In addition to compression testing, creep testing was performed over a 90-day period with negligible loss in measured force; this loss in force was more likely due to a non-control temperature environment.

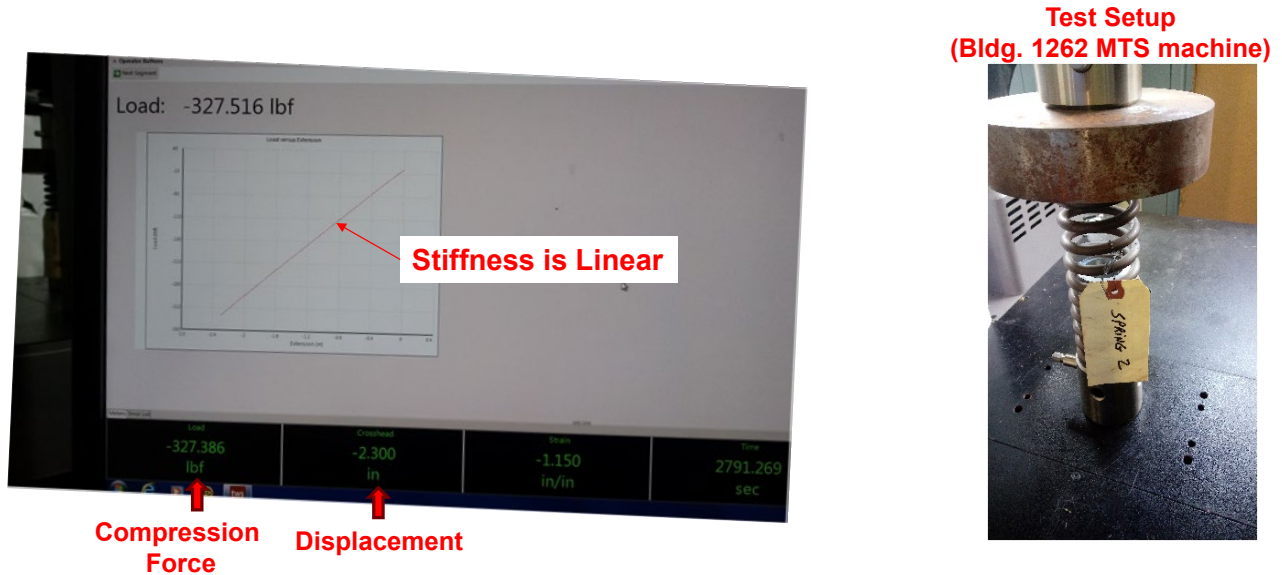


Figure 14. Compression Spring Test Results (Left); Creep Testing Setup (Right)

Developmental functional testing was used to characterize the design and to estimate friction losses in the system. High speed video was utilized to capture the velocity and height of the EDM after 2 meters of travel (the distance to outer surface of the RV aeroshell). The ejection mechanism assembly was mounted to a test stand with white contrasting backdrop setup on partitions. A line was measured and drawn out at 2 meters using black tape on the backdrop to mark the end of the aeroshell and a curtain was setup to catch the EDM after ejection at the end of each test, Figure 15.

Figure 15. Functional Test Setup



Velocity and height measurements were derived from the high-speed video captures. Velocities were measured just after ejection exit and at the 2-meter mark. Height was also measured at the 2 meters

mark, Figure 16. These numbers were compared to the theoretical numbers and friction loss of the system was derived. An energy loss of around 25% was derived which was a little more than anticipated for the system.

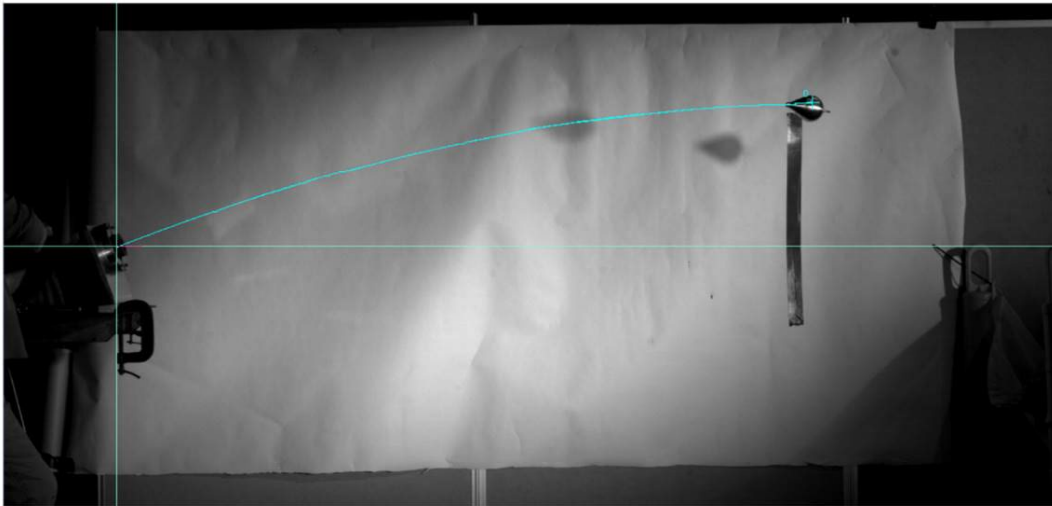


Figure 16. High-Speed Video Clip

After functional testing, the mechanism was subjected to random vibration testing. While testing, an anomaly occurred resulting in a premature release of the mechanism. Immediate findings showed that the NEA threaded stud broke and a guide dowel pin had been liberated from the mechanism assembly, Figure 17.

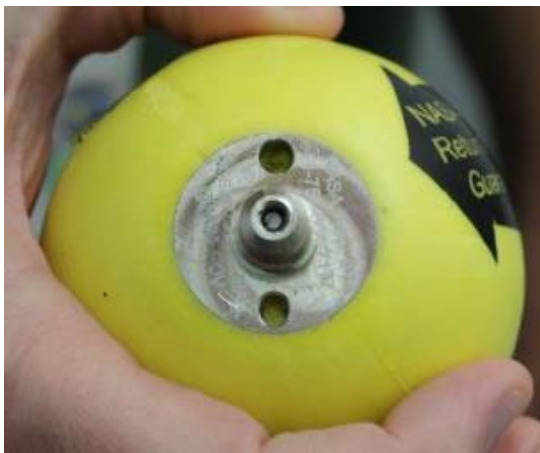


Figure 17. Broken Threaded Stud (Left); Liberated Dowel Pin (Right)

Further investigations showed that the threaded stud failed by fatigue. The fracture started, travelled about 40% of the surface and then the morphology changed. The fracture then travelled another 10% before the stud completely broke. The belief is the morphology change was from the dowel pin liberating itself from the assembly. Investigating the dowel pin revealed the pin and its mating hole were covered in dry film lubricant, Figure 18. It appeared that the dowel pin hole was not thoroughly cleaned before pressing the pin in place.



Figure 18. Lubricant on Pin (Left). Lubricant Wiped (Center). Lubricant in Hole (Right)

From this anomaly, a redesign effort was made to reduce cycling on the threaded stud and to retain the three guide pins. A custom flanged bushing was added between the pusher and the EDM to reduce movement in the NEA threaded stud, Figure 19.

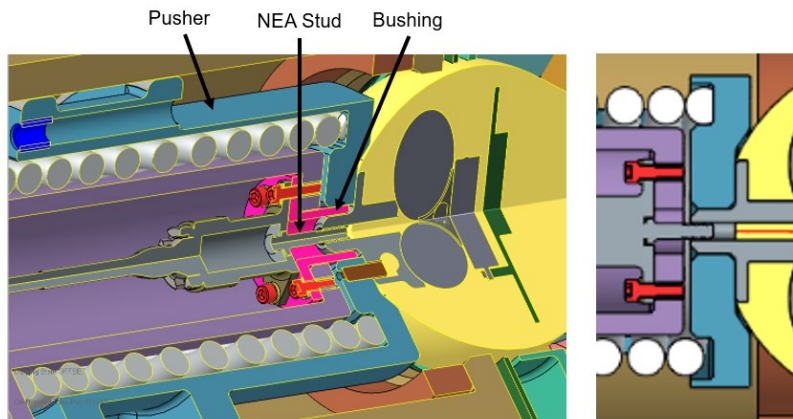


Figure 19. Added Bushing (Left). Previous Design (Right)

Retention plates were also added to keep the three guide pins from backing out of the pusher. Figure 20.

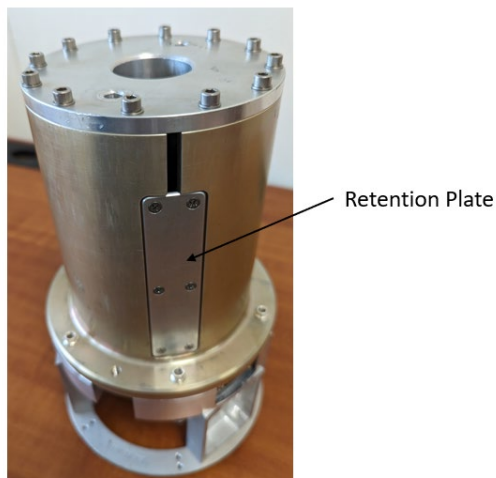


Figure 20. Retention Plate

The addition of the bushing introduced more friction into the system so some mass was machined out of the pusher to compensate.

The updated mechanism design was then run through its qualification tests successfully. These tests included functional and performance, random vibration, thermal vacuum, and maximum/minimum temperature firings. As shown in Figure 21, the velocities were very predictable and consistent at room temperature, so the expected standard deviation is small. In Figure 22, AT-017 was not clamped to the stand, therefore energy was lost in the recoil to the EDR. The resultant velocity was below the minimum needed for a positive force margin forcing a risk to be introduced to the project. The risk would be the EDM not clearing the RV during flight and the risk was deemed low.

Test	Test ID Number	Velocity (ft/sec)
1	AT-001	27.30
2	AT-002	27.30
3	AT-003	27.30
4	AT-004	27.30
5	AT-005	27.50
6	AT-006	27.30
7	AT-007	27.50
8	AT-008	27.30
9	AT-009	27.30
10	AT-010	27.50
11	AT-011	27.20
12	AT-012	27.50
13	AT-013	27.50
14	AT-014	27.40
15	AT-015	27.40

Minimum Velocity, v_{min}	27.20	ft/s	= $Min(Test\ 1\ through\ Test\ 15)$
Maximum Velocity, v_{max}	27.50	ft/s	= $Max(Test\ 1\ through\ Test\ 15)$
Average Velocity, v_{avg}	27.37	ft/s	= $Sum(Test\ 1\ through\ Test\ 15) / No.\ of\ Tests$
Standard Deviation, σ_{vel}	0.10	ft/s	= $stdev.p(Test\ 1\ through\ Test\ 15)$
2 σ Minimum Velocity, $v_{min\ projected}$	27.17	ft/s	= $v_{avg} - 2 * \sigma_{vel}$

Figure 21. Run-In Testing (Flight Unit)

Test	Test ID Number	Velocity (ft/sec)	Comments
1	AT-016	29.30	Ejection performed after TVAC and Vibing
2	AT-017*	26.30	Hot-Temperature Ejection
3	AT-018	31.90	Cold-Temperature Ejection

- AT-017 velocities were low due to recoil (the test fixture was not clamped).

Figure 22. Run-In Testing (Flight Unit)

Flight Ejection

The ejection mechanism successfully ejected the EDM during reentry, clearing the RV, and splashing down in the Pacific Ocean, Figure 23. The EDM landed approximately 6 miles from the recovery ship and was retrieved. Data was successfully extracted from the EDM as well.

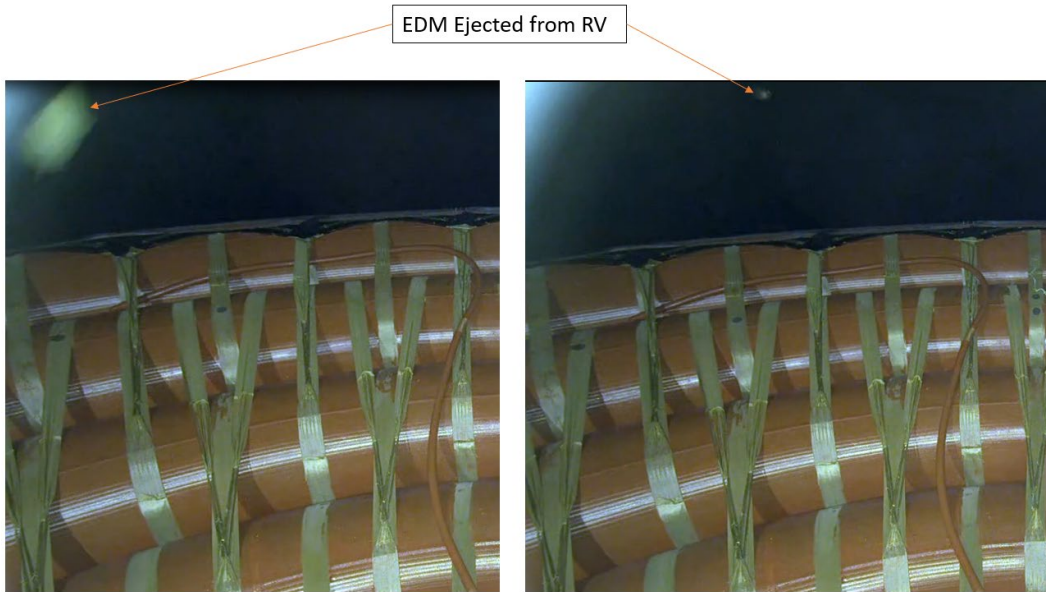


Figure 23. EDM Ejecting from RV

Conclusion

The EDR ejection mechanism had a few challenges throughout its development but ended up being successful. Through development testing, friction was found to be greater than anticipated which reduced the ejection velocity and forced the team into evaluating the risk of having a negative force margin. In lieu of relying on published data for low-friction coating such as tungsten disulfide, a test program to develop friction coefficients for this configuration would have been invaluable. The EDR ejection mechanism is currently being looked at for future HIAD flights as a secondary data recovery system.